DIFFUSION FLAMES AND SUPERSONIC COMBUSTION

BY

I. DA-RIVA
E. FRAGA
A. LIÑAN
J. L. URRUTIA

INSTITUTO NACIONAL DE TECNICA AEROESPACIAL
«ESTEBAN TERRADAS»

MADRID (SPAIN)
October 1, 1966

A B S T R A C T

The paper describes some analytical work connected with the purely diffusive mode of supersonic combustion.

The basic problems considered have been: the study of the hydrogen-air diffusion flames, under both close to and far from equilibrium conditions, and the study of the aerodynamic field near the injector exit when the ratio of injected to outer total pressures is small.

The internal structure of hydrogen-oxygen diffusion flames close to equilibrium has been studied using the first order approximation of an asymptotic expansion method, in which the large parameter represents the ratio between a characteristic mechanical time and a chemical time.

Far from equilibrium conditions, the above mentioned solution fails. However, when a free jet of hydrogen, parallel to the air stream is used for injection purposes, a very simple near frozen approach may be used. The main simplifying features of such an approach being; the use of an overall chemical reaction, the assumption that fuel and oxidizer mix without appreciable depletion and chemical heat release, and the linearization of the mixing problem.

Finally a discussion of some means of improving the mixing process, near the injector exit, is made, using some experimental evidence from work on related problems by other groups.

- - - - - - - -

TABLE OF CONTENTS

= = = = = = = = = =

INTRODUCTION

In recent years considerable attention has been devoted to the study of supersonic combustion in order to develop a hypersonic air-breathing vehicle in which the entering stream would be slightly decelerated, so that large increases of static temperature and losses associated with the deceleration are avoided. In the combustion system of such a vehicle the very rapid mixing and burning of fuel in the air stream is intended. The propulsion system using this form of combustion is called SCRAMJET (Supersonic Combustion Ramjet).

It appears that SCRAMJET propulsion would make it possible to place heavy loads in orbit, by powering the atmospheric stage with this form of propulsion and using lighter, smaller, and more maneuverable vehicles than would be feasible with rocket propulsion. Furthermore, present results show that direct operating costs for ramjet powered hypersonic airplanes would not be greater than for the supersonic transport.

Among all the proposed systems of supersonic combustion, the purely diffusive mode is the one which fits better to the large flight Mach numbers ($6 \leq M \leq 25$), since a small deceleration of the flow may be enough to increase the pressure and temperature, so that fuel and oxidizer react as soon as they contact.

Diffusive supersonic combustion presents very challenging basic problems, due to the incomplete state of knowledge in some related areas such as chemical kinetics and turbulent mixing of gases, especially gases of very different densities. Certain aspects of these problems have been studied analytically under the reported Grant, with the set up to contribute to the efficient use of digital computers in the study of more complicated and realistic configurations, and to a rational interpretation of experimental results.

The basic problems considered have been: the study of the hydrogen-air diffusion flame, in both close to and far from equilibrium conditions; and the study of the aerodynamic field

near the injector exit when the ratio of injected to outer total pressures is small. It has always been assumed that the injection is parallel to the main flow direction.

Regarding diffusion flames close to equilibrium,it may be shown that when the flow temperature and pressure are large enough and the gradients of the concentration of species are not too large,the characteristic chemical time for the chemical reaction to take place is much smaller than the diffusion time, so that it is possible to solve the problem using an asymptotic expansion method, the large parameter being the ratio between the characteristic mechanical time and the chemical time. Under the first order approximation, the continuity equations for the different species, which are ordinary differential equations, have been solved using an integral method.

The calculation show that, in the case of hydrogen-oxygen chemical kinetics,under conditions considered, the fast reactions are close to equilibrium,while in the neighborhood of the zone of maximum reaction rate, the recombination reactions play an insignificant role.

The above mentioned solution fails when the conditions are not so close to equilibrium. However, near the injector exit where temperature is not large enough to give rise to significant reaction rates a near-frozen approach may be used. This approach is based on the fact that, at least in the case of Hydrogen-Oxygen kinetics, the chain initiation reactions are very slow, hence it is possible to assume that fuel and oxidizer mix without appreciable concentration change and heat release resulting from the chemical reactions. Nevertheless, radicals, mainly H , are produced. The zone ends when the H concentration has reached a sufficiently large value,triggering the fast "shuffling" reactions.

The most significant result from this part of the study is that the length of this zone is extremely sensitive to an uncontrolled (or provoked) initial presence of radicals.

The last part of the undertaken study concerns the

feasibility of improving aerodynamically the mixing process and hence to disminish the ignition delay, without appreciably disturbing the outer flow.

Some experimental evidence from other research groups, seems to indicate that when the ratio of injected to outer total pressures is small, (as is the case when hydrogen is used as fuel) a wakelike configuration appears near the injector exit.

In those cases in which the recirculation length is comparable to the ignition delay for the chemical reaction, recirculation sends radicals backwards, and those radicals in contact with the hydrogen jet trigger the fast reactions.

The coupling of this phenomenon with some radical producing effect (such as dissociation in the injector outer boundary layer, electrical discharges, etc.) seems to be worth of more extensive analytical and experimental research.

The aim of this paper is both to summarize the work previously published by the group under the reported period, and to present some yet unpublished additional work.

1. HYDROGEN AIR DIFFUSION FLAME CLOSE TO EQUILIBRIUM

When flying at high Mach numbers in the atmosphere, within the range proposed for SCRAMJET powered vehicles, the static temperature and pressure in the combustor may be sufficiently large as to make chemical time small compared to the characteristic mechanical time. In that case, the reaction is a diffusion controlled one throughout the combustion chamber except near the injector exit, and takes place in a very thin region.

A solution of the problem, obtained by assuming infinitely fast reaction rates, has been known since long ago: the "thin flame" or Burke-Schumann equilibrium solution[1]. This solution is not uriformly valid because concentration and temperature derivatives normal to the flame surface are discontinuous at the flame. These discontinuities, which are due to

the fact that. in the limiting process, the reaction region shrinks to a sheet, indicate that transport terms play a dominant role in the combustion zone of the large, although finite, reaction rate case.

The infinitely fast reaction solution, may be viewed as the outer solution" of our problem, useful to calculate the flame position, fuel consumption per unit flame area, and to provide the outer boundary conditions for the "inner problem".

From the solution of this 'inner problem' we get a criterion for the existence of an infinitely thin flame. Such a thin flame seems to be desirable from the combustion efficiency point of view.

The study presented here, allows us to calculate, to the first order in a small parameter representing the ratio between a characteristic chemical time and a mechanical time, the distribution of species across the flame for a quite general set of outer solutions. But higher order terms should be calculated to account for flames not too close to equilibrium.

1A. Structure of the Diffusion Flames

In order to introduce the method used to study the internal structure of the diffusion flames, we will confine ourselves to the equations expressing the conservation of reactants and intermediate species, which are the only ones containing explicitly the small parameter involved. Reference is made to [2] for more complete details on the method.

The said equations are, under the boundary layer approximation:

$$u \frac{\partial Y_i}{\partial x} + v \frac{\partial Y_i}{\partial y} = \frac{1}{Re} \frac{1}{\rho} \frac{\partial}{\partial y} \left[\frac{\mu}{Sc} \frac{\partial Y_i}{\partial y} \right] + \frac{1}{d} \frac{w_i}{\rho} \qquad (1)$$

where

$Re = VL \rho_o / \mu_o$ is the Reynolds number

$Sc = \mu / \rho D$ is the Schmidt number

$d^{-1} = LU/V$ is the first Damköhler parameter

V, L, ρ_o, μ_o are characteristics magnitudes, and U a charac-

teristic reaction frequency. The remaining variables are non-dimensional. d^{-1} represents the ratio of a mechanical time to a chemical time.

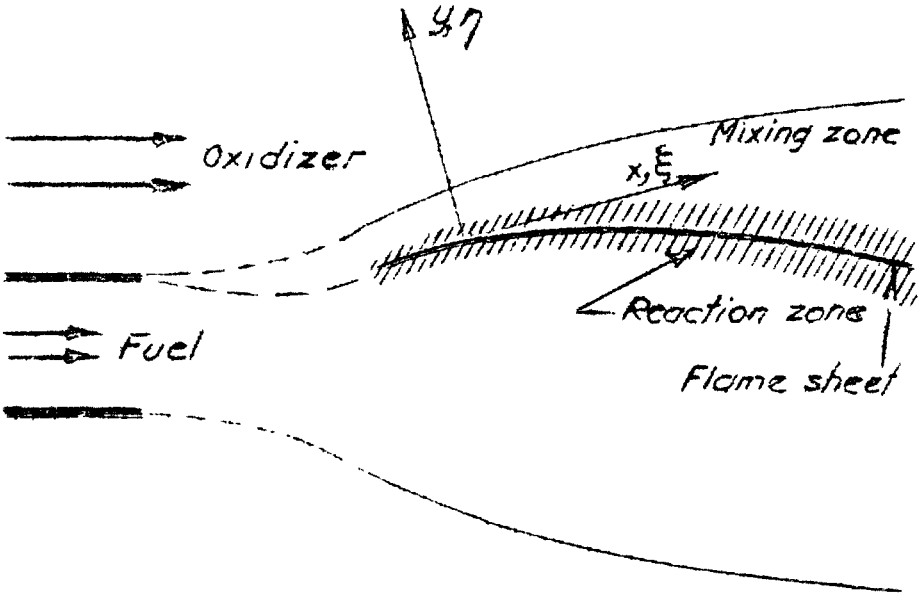

Fig.1. Reference Coordinate System for the Near-Equilibrium Diffusion Flame.

The mass concentration Y_p of products is obtained by using the expression

$$\Sigma Y_i = 1 - Y_N$$

where Y_N is the mass concentration of inert species.

It is assumed that (1) is valid in the turbulent case, when using mean values of the appropriate magnitudes and turbulent transport coefficients.

According to the usual boundary layer approximation, the mixing layer thickness δ_m is of order L/Re^n ($n = 1/2$ in the laminar case and $n = 1/5$ for turbulent flow). y and v are of the same order, while x, u, ρ, Y_i, and the temperature T are of order unity.

In the limiting case of infinite reaction rate, the solution presents the following peculiarities:

a) The thickness of the reaction zone is zero.

b) Concentrations of intermediate species are zero everywhere, while the concentration of oxidizer is zero at the fuel

side of the flame and concentration of fuel is zero at the oxidizer side(*).

c) The first derivatives of the principal species and temperature normal to the flame are discontinuous there.

The above mentioned peculiarities suggest us that in the case of very large although finite values of d^{-1}, the following properties hold in the reaction zone.

a) The thickness δ_c of the zone is very small. y/δ_c is of order unity.

It must be pointed out that, although the Reynolds number is usually fairly large, we assume $\delta_c/\delta_m \ll 1$, so that in problems such as diffusive combustion in a boundary layer or a free mixing layer, the reaction zone thickness is smaller than the boundary layer, or mixing layer, thickness. This happens to be true in cases of technical interest[3].

b) The concentrations of reactants and intermediate species are of order δ_c/δ_m, but the mass fraction of products Y_p and inert species Y_m are of order unity.

c) The diffusion terms will balance the chemical production terms.

Since for a second order chemical kinetics, the reaction terms are of order $d^{-1}(\delta_c/\delta_m)^2$ and the diffusion terms of order $\delta_m^{\frac{1-n}{n}}/\delta_c$, we conclude that the non-equilibrium zone thickness δ_c must be order $d^{1/3}\,\delta_m^{n+1/3n}$ ($n = 1/2$ or $1/5$

(*) This paragraph deserves more careful analysis when dissociation-recombination reactions, such as

$$H + H + X \rightleftharpoons H_2 + X$$
$$O + O + X \rightleftharpoons O_2 + X$$
$$H + OH + X \rightleftharpoons H_2O + X$$

or chain initiation reactions, like

$$O_2 + O_2 \rightleftharpoons O_3 + O \quad ,$$

play an important role in the zone considered, since these reactions do not reach equilibrium under conditions stated in b). In this study we will confine our attention to the zone where the fast reactions are so far from equilibrium that the dissociation-recombination or initiation reactions play a purely marginal role.

depending on whether the mixing layer is laminar or tubulent).

Using the usual technics to write the first order inner equations in the method of "matched asymptotic expansions" [4], we introduce magnified inner concentrations $J_i = Y_i(\xi,\eta)/d^{1/3}\delta_m^{1-2n/3n}$ where $\xi = x$, $\eta = y/d^{1/3}\delta_m^{n+1/3n}$, obtaining the following conservation equations for reactants and intermediate species:

$$\frac{1}{Re}\ \frac{1}{\rho}\ \frac{d}{d\eta}\left[\frac{\mu}{Sc}\ \frac{dJ_i}{d\eta}\right] = -\frac{w_i}{\rho} \quad . \qquad (2)$$

On the other hand, equations (1) reduce to $w_i = 0$ in the outer zone, indicating that the outer problem is an equilibrium mixing one. Its solution gives the position and characteristics of the "flame sheet". These characteristics, which are the outer boundary conditions of the inner problem being: $\rho = \rho_f(\xi)$, $u = u_f(\xi)$, $v = v_f(\xi)$, $T = T_f(\xi)$, $Y_p = Y_{pf}(\xi)$, $Y_R = 0$, at either side of the flame (subscript f means equilibrium conditions at the flame sheet, and subscript R means radical). In addition, at the fuel side of the flame, $Y_o = 0$, $dY_F/d\eta = A_F(\xi)$ (o and F mean respectively oxidizer and fuel); at the oxidizer side $Y_F = 0$, $dY_o/d\eta = A_o(\xi)$. The A are also computed from the solution of the outer problem.

The equations (2), which are ordinary differential equations, give the distribution of species across the reaction zone. In addition, since the temperature is close to the adiabatic flame temperature and, neglecting higher order terms, may be taken as constant across the flame, the problem of computing the reaction rate is greatly simplified.

1B. Hydrogen-Oxygen Chemical Kinetics

The following individual steps and reaction rates are widely used in supersonic hydrogen-air combustion evaluation studies[5].

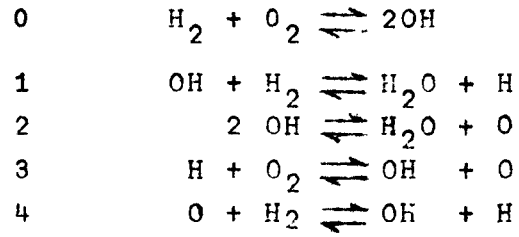

$$5 \qquad H + H + X \rightleftharpoons H_2 + X$$
$$6 \qquad O + O + X \rightleftharpoons O_2 + X$$
$$7 \qquad H + OH + X \rightleftharpoons H_2O + X$$
$$8 \qquad O + H + X \rightleftharpoons OH + X$$

The symbol X denotes any third body.

Writing the rate constants of the forward (K_j) and reverse reactions (K_{-j}) in the form

$$K_j = k_j \, e^{-E_j/RT}$$

we condense, the pertinent values in Table I.

T a b l e I

j	k_j	k_{-j}	E_j	E_{-j}
0	10^{14}	2×10^{13}	7×10^4	6.12×10^5
1	3×10^{14}	1.2×10^{15}	6×10^3	2.06×10^4
2	3×10^{14}	3.12×10^{15}	6×10^3	2.49×10^4
3	3×10^{14}	2.7×10^{13}	1.75×10^4	3.3×10^4
4	3×10^{14}	1.3×10^{14}	8×10^3	6×10^3
5	10^{16}	$7.27 \times 10^{18} T^{-1/2}$	0	1.1×10^5
6	10^{15}	$3.16 \times 10^{19} T^{-1/2}$	0	1.32×10^5
7	10^{17}	$3.06 \times 10^{22} T^{-1}$	0	1.15×10^5
8	10^{16}	$3.16 \times 10^{18} T^{-1/2}$	0	1.07×10^5

The temperatures are in °K , the rate constants are given in $(\text{mole/cc})^{-1}$ sec^{-1} for second order reactions, and in $(\text{mole/cc})^{-2}$ sec^{-1} for third order reactions, and the activation energies in cal/mole °K. The role of reactions 0 and 5 to 8 is purely marginal in the diffusion flame zone, since H_2 and O_2 do not coexists in appreciable amounts within the flame, and the concentrations of radicals are very small.

1c. Structure of the Hydrogen-Air Diffusion Flames

The above mentioned kinetic scheme has been used to study the internal structure of the Hydrogen-Air Diffusion Flames. Nitrogen is treated as an inert diluent. This assumption seems to be valid for temperatures below roughly 2500°K.

The species being produced or destroyed are: H_2O , H_2 , O_2 , HO , H , and O , denoted respectively by subscripts 1 to 6.

Within the reaction zone, assuming constant values of $\rho^{\alpha}\mu$ and Schmidt number, the conservation equations for the principal species and radicals become:

$$\frac{d^2}{d\bar{y}^2} \frac{Y_i}{m_i} = F_i \quad , \tag{3}$$

where,

$$\bar{y} = \int_0^y \left[\frac{\rho\ (x,\ y)}{\rho\ (x,\ 0)} \right]^{\alpha} dy \quad ,$$

m_i is the molecular weight of species i , and the F_i are known functions of pressure, temperature, the mixing parameters of the outer flow,and the yet unknown concentrations. The boundary conditions are:

Fuel side $\bar{y} = -\infty$

$$\frac{d}{d\bar{y}} Y_2 = - \frac{d}{d\bar{y}} (Y_1 + Y_N) = - A \ ; \ \frac{d}{d\bar{y}} Y_i = 0 \quad i=3,4,5,6 \tag{4}$$

Oxidizer side $\bar{y} = +\infty$

$$\frac{d}{d\bar{y}} Y_3 = - \frac{d}{d\bar{y}} (Y_1 + Y_N) = 8A \ ; \ \frac{d}{d\bar{y}} Y_i = 0 \quad i= 2,4,5,6 \tag{5}$$

Equations (3) with boundary conditions (4) and (5),have been approximately solved by using an integral method.

Let us consider, for instance,the equation corresponding to depletion of hydrogen molecules.

If we introduce a straining parameter $\delta_2\ (x)$ such that $\eta_2 = \bar{y}/\delta_2$ is of order unity throughout the reaction zone, the following approximate equation holds:

$$\frac{d^2}{d\eta_2^2} \frac{Y_2}{m_2} = \delta_2^2\ F_2(\eta_{o2})\ \ e^{-(\eta_2 - \eta_{o2})^2} \tag{6}$$

η_{o2} is the point where the depletion term of molecular hydrogen reaches its maximum.

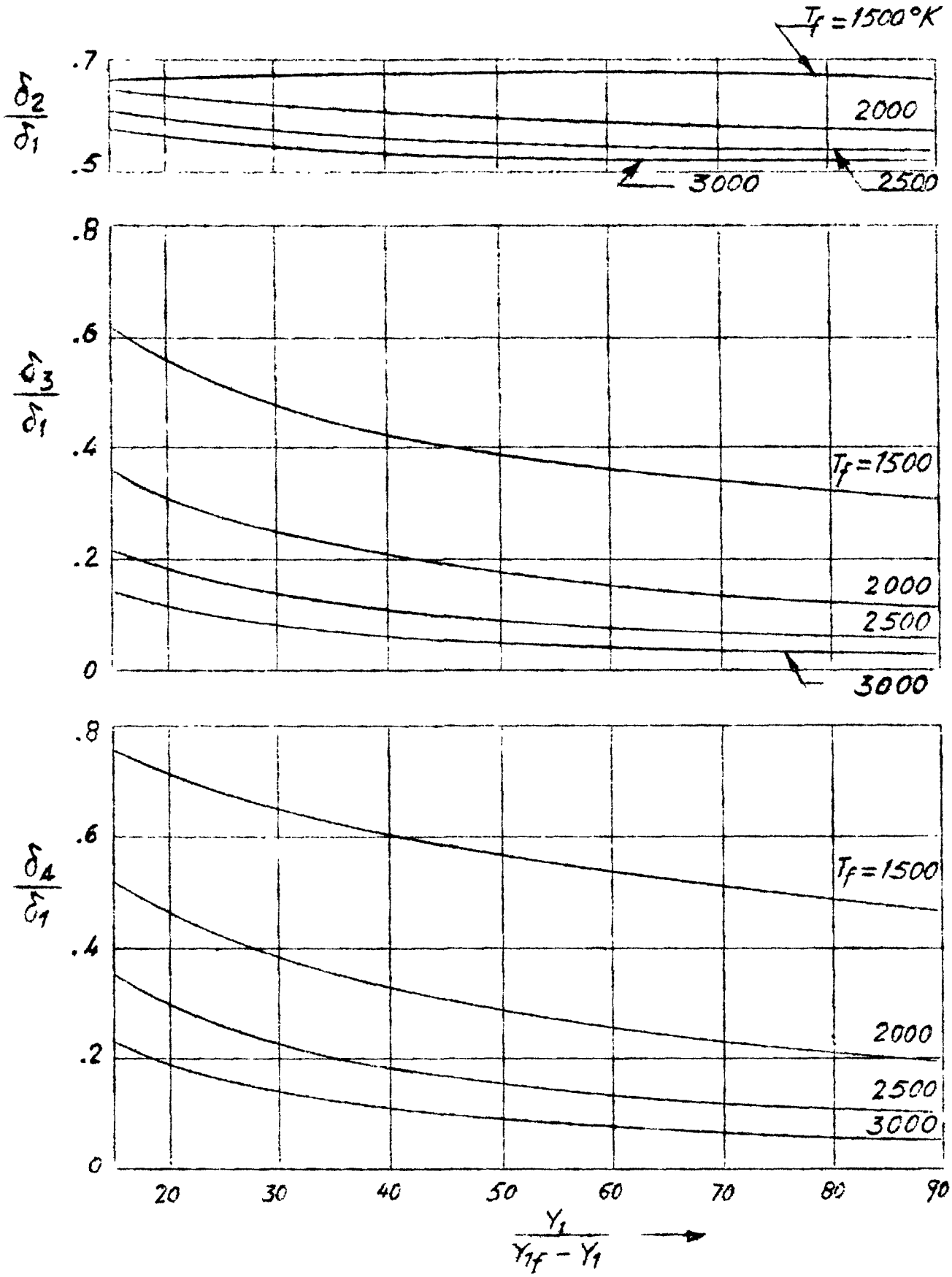

Fig 2. Parameters indicating the thickness of the different non-equilibrium zones.

The boundary conditions are:

$$\text{Fuel side} \qquad \eta_2 \to -\infty \qquad Y_2 \to -A\,\delta_2\eta_2 \tag{7}$$

$$\text{Oxidizer side} \qquad \eta_2 \to +\infty \qquad Y_2 \to 0$$

Integrating twice (6) with conditions (7) we deduce the following relations:

$$\eta_{o2} = 0 \tag{8}$$

$$A = 2\,\delta_2\,\sqrt{\pi}\,F_2\,(0) \tag{9}$$

$$\frac{Y_2}{m_2} = \frac{A}{4}\,\delta_2\left[\frac{1}{\sqrt{\pi}}\,e^{-\eta_2^2} - \eta_2\,(1 - \operatorname{erf}\eta_2)\right] \tag{10}$$

where

$$\operatorname{erf}\eta_2 = \frac{2}{\sqrt{\pi}}\int_0^{\eta_2} e^{-x^2}\,dx$$

Following a similar way, we get the expressions giving the distributions of Y_1/m_1 , Y_3/m_3 and $Y_1/m_1 + Y_4/m_4$,while the distributions of Y_5/m_5 and Y_6/m_6 may be expressed as functions of Y_1 , Y_2 , Y_3 and Y_4 by writing two linear relations which are independent of the chemical reactions.

In order to calculate the four straining parameters δ_i , we write the $F_i(\eta_{oi})$, by means of the law of Mass Action and the chemical kinetic scheme considered in § 1B , as functions of pressure, temperature, and the concentration of species calculated above for $\eta_i = \eta_{oi}$.

The final solution is obtained with the aid of figures 2 and 3 . In figure 2 the relations δ_i/δ_1 , $i = 2,3,4$, have been plotted versus the ratio $Y_1/Y_{1f} - Y_1$, where subscript f means equilibrium conditions at the flame sheet; figure 3 connects the inner and outer solutions, in the following way : The solution of the outer problem provides the value of A ,

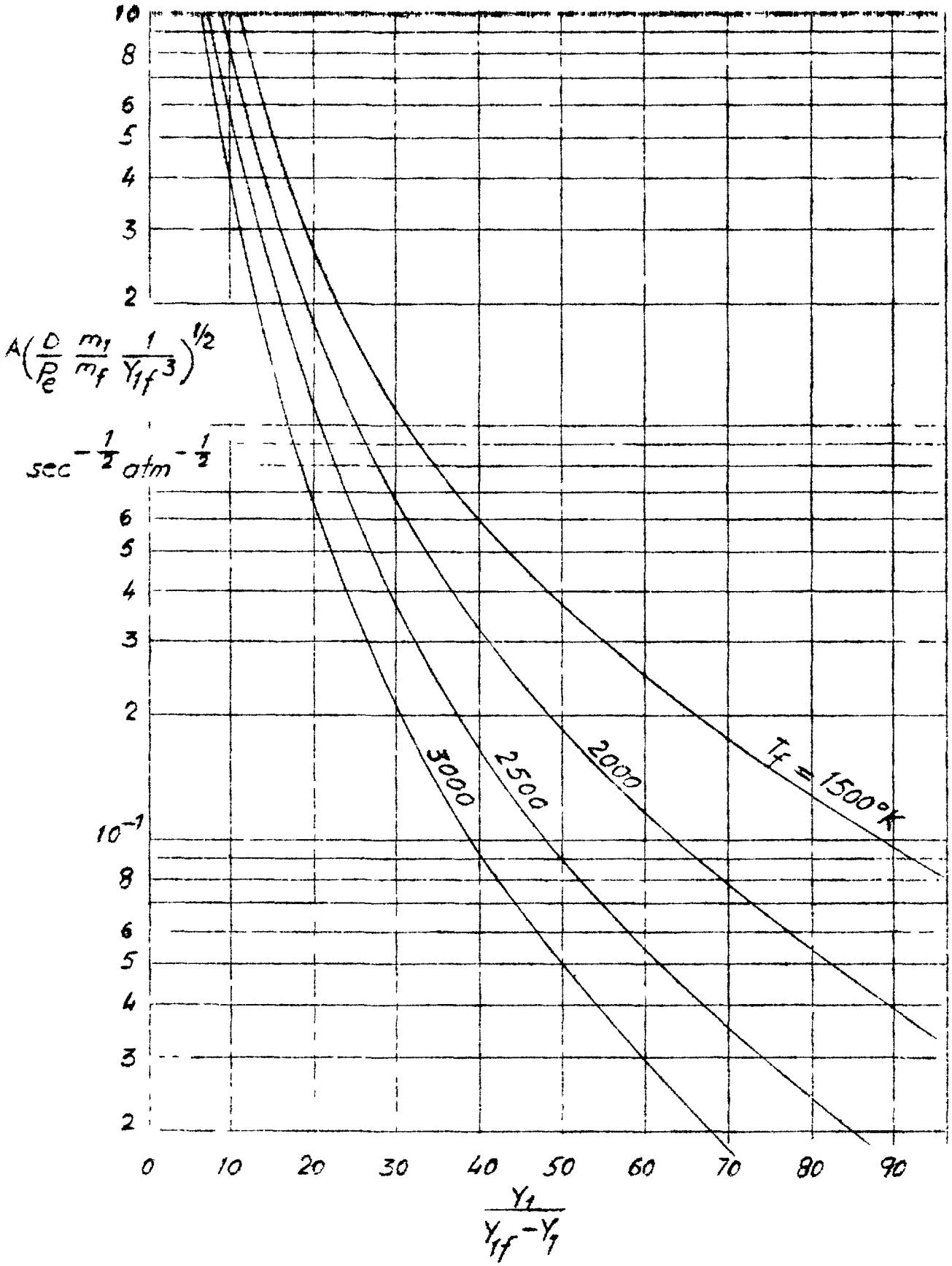

Fig.3. Relation between outer conditions and non equilibrium water concentration in the flame sheet.

D (diffusion coefficient), p_e , m_f (mean molecular weight at the flame sheet), Y_{1f} and T_f , so that by using this figure we get $Y_1/Y_{1f} - Y_1$, and from figure 2 we deduce the ratios δ_i/δ_1 . Finally an equation similar to (10) but involving $Y_{1f} - Y_1$ and particularized at $\eta_1 = 0$ gives us the value of δ_1.

Some of the reaction rates involved have been represented in figure 4. From this figure we deduce that the dissociation-recombination reactions do not play a significant role in the zone considered, at least near $\eta = 0$ where these rates have been computed. This is in agreement with what it has been assumed throughout this study. On the other hand, the fact that reactions 1 , 2 and 4 do not depart substantially from equilibrium as seen from this figure, may be used to arrive at a simpler description of the chemical kinetics involved.

2. THE IGNITION DELAY REGION IN DIFFUSIVE SUPERSONIC COMBUSTION

The near-equilibrium treatment of the diffusion flames is no longer valid close to the injector exit where, owing to the large concentration gradients and low temperatures involved, diffusion and chemical times are of the same order of magnitude. Nevertheless a very simple approach may be used in this region. The main simplifying features of such an approach are: the use of an overall chemical reaction, the assumption that fuel and oxidizer mix without appreciable concentration change and heat release resulting from chemical reaction, and the linearization of the mixing problem following essentially the approach taken to study the turbulent jet mixing between two streams at constant pressure by Korst et al.[6]

2A Chemical Kinetic Scheme in the Ignition Delay Region

The temperature of the incoming air stream is, in the cases of interest to supersonic burners, of the order of 1200°K and the pressure of one atmosphere. Lower temperatures and pressures would give rise to large ignition delays. On the other hand, if the air static temperature at the injector

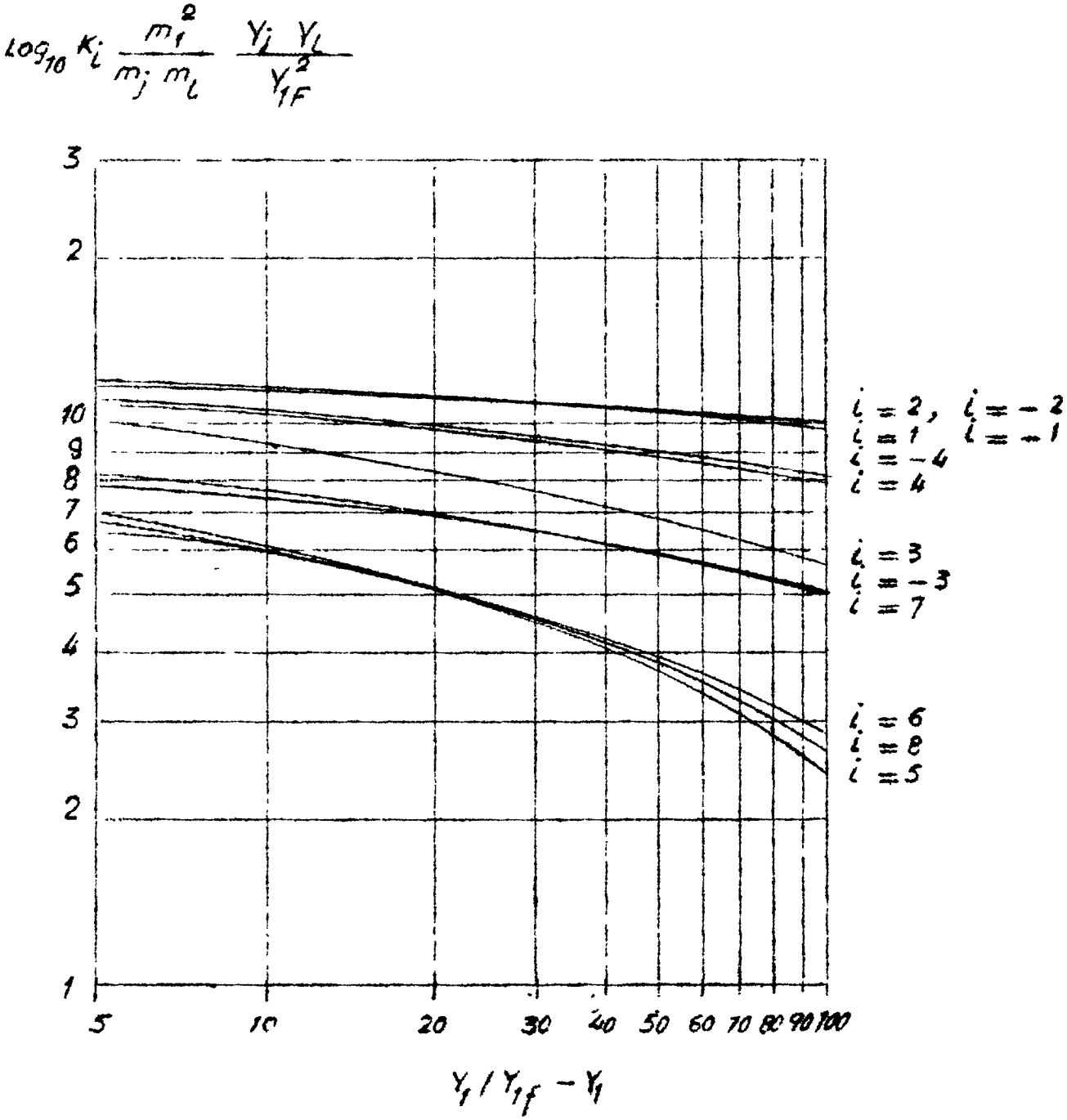

Fig 4. Reaction rates in the study of the diffusion hydrogen-air flame structure, p_e = 1 atm. T_f = 2500°K.

exit is much larger than the above mentioned value, the final combustion temperature will be too high and the products would leave the combustor with a large amount of dissociation.

For these temperatures and pressures, the chemical kinetic scheme is reduced to the following elementary processes

$$0 \quad H_2 + O_2 \longrightarrow 2\ OH$$
$$1 \quad OH + H_2 \longrightarrow H_2O + H$$
$$3 \quad H + O_2 \longrightarrow OH + O$$
$$4 \quad O + H_2 \longrightarrow OH + H$$

The role played by the remaining reactions of the more complete kinetics is purely marginal owing to their small specific reaction rates, and the low concentration of intermediate and final species involved.

The rate constant of the chain initiation reaction 0 is very small, so that this reaction is responsible for the large ignition delays appearing in the hydrogen-oxygen combustion processes. When there is an appreciable amount of radicals, H , OH or O , initially present either in the air or in the fuel streams, the initiating reaction may become unimportant; otherwise, it is the only initiation process ocurring in practice under conditions relevant to supersonic combustion studies.

In addition, the forward rate constants of 1 and 4 are higher than the constant corresponding to the forward reaction 3 . Hence we may assume that in most of the ignition delay region:

1^{st}. Any amount of O initially present will be converted by means of the fast reaction 4 into OH and H .

2^{nd}. Similarly, any OH initially present or produced by the reactions 0 or 4 , will be immediately depleted by the reaction 1 , producing H_2O and H .

3^{rd}. The OH atoms produced by the relatively slow reaction 3 , will be soon converted into H and H_2O by means of the reactions 1 and 4.

Summarizing, if for any reason (such as dissociation in the injector outer boundary layer) some concentration of atomic oxygen is initially present near the injector, we may assume that each atom of oxygen reacts inmmediately with two molecules of H_2 producing two atoms of H and one molecule of H_2O . Similarly, each mole of OH gives rise to one mole of H and one mole of H_2O . Hence, the set of processes 0 , 1 , 3 and 4 may be substituted by the over-all reaction

$$3H_2 + O_2 \longrightarrow 2H_2O + 2H$$

obtained combining 0 , 1 , 2 and 4 in such a way that neither O nor OH will appear as reactants or products.

The over-all production rate of H is :

$$\frac{w_5}{m_5} = \frac{w_1}{m_1} = 2K_o\rho^2 \frac{Y_2}{m_2} \frac{Y_3}{m_3} + 2K_3\rho^2 \frac{Y_3}{m_3} \frac{Y_5}{m_5} \qquad (11)$$

Once a sufficient number of hydrogen atoms has been produced,the various reactions occur rapidly and exothermally so that the temperature begins to increase and the concentrations of the main reacting species H_2 and O_2 begin to decrease.However, the structure and boundaries of the ignition delay region may be determined assuming, as a first order approximation, that fuel and oxidizer mix without concentration change and heat release resulting from the chemical reaction.

There are many criteria to define the end of the ignition delay zone. One could use as a criterium that the reverse reaction 1 should be of the same order as the forward reaction 3. Afterwards the amount of OH and O would grow rapidly until a partial equilibrium would be attained.

2B. Simplified Formulation of the Mixing Problem

A considerable amount of effort has been devoted in the past to the study of jet mixing. Our analysis of the turbulent free mixing layer between two streams follows essentially the approach advanced earlier by Korst et al[6] to deal with the mixing between one stream and the quiescent fluid. Since this model

may be useful in problems involving flow separations and fully separated wake-like flows, it has been the subject of recently renewed interest.[7]

In the case considered, of low speed parallel hydrogen-injection in a supersonic stream, the mass and momentum injection rates are very low, so that it seems logical to assume that this injection does not appreciably disturb the wake-like configuration, and a treatment similar to that considered by Korst may be used to describe the fluid dynamic aspects of the problem. Such a treatment takes into account the following phenomena: expansion around the injector exit, turbulent mixing at constant pressure alongthe wake boundaries, pressure rise at the neck, and mass conservation inside the wake.

In the present section we are particularly concerned with the isobaric mixing mechanism between the two streams.

We may write the equation of motion in the following form:

$$u \frac{\partial u}{\partial x} + v \frac{\partial u}{\partial y} = \varepsilon \frac{\partial^2 u}{\partial y^2} \qquad (12)$$

where ε is the (apparent) eddy diffusivity for the turbulent flow.

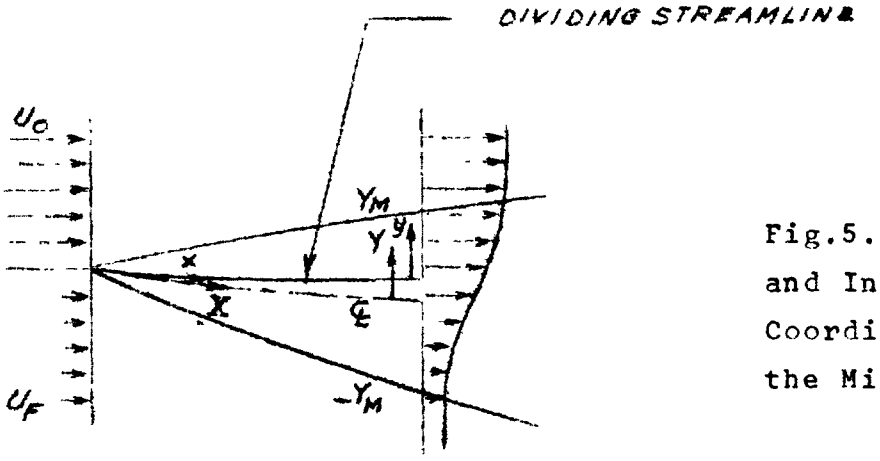

Fig.5. Reference (X , Y) and Intrinsic (x , y) Coordinate Systems for the Mixing Zone.

In the analysis by Korst, a linearized equation of motion is solved, resulting in the velocity profile equation

$$u = \frac{u_o + u_F}{2} + \frac{u_o - u_F}{2} \operatorname{erf} \eta \qquad (13)$$

where

$\eta = \sigma\, y/x$

σ a similarity parameter

u_o , u_F undisturbed velocities in either side of the free mixing zone

$$\operatorname{erf} \eta = \frac{2}{\sqrt{\pi}} \int_o^{\eta} e^{-\beta^2} d\beta$$

Because of the many simplifications in the equation of motion, the velocity and temperature fields are interpreted to hold in an intrinsic system of coordinates (x, y). The intrinsic coordinate system is shifted in the Y direction from the physical coordinates (X , Y) accordingly

$$x = X$$

$$y = Y + y_m(x)$$

where $y_m(0) = 0$ (See Fig.5).

The orientation of the intrinsic system of coordinates with respect to the physical system is accomplished by using a momentum integral equation.

The effect of the injector boundary layers on the velocity profiles in the free shear layer has been neglected, otherwise eq.(13) is not valid very near the injector exit.

Consistently with this approximation, we write the equations of conservation of species in the following form:

$$\frac{\partial^2 Y_i}{\partial \eta^2} + 2\eta \frac{\partial Y_i}{\partial \eta} = - \left[\frac{4}{\varepsilon} \int \frac{\varepsilon}{U} dx \right] \left[\frac{w_i}{\rho} - U \frac{\partial Y_i}{\partial x} \right] \qquad (14)$$

Here, as in the momentum equation, it has been assumed that v is negligible and that u can be approximated by $U = (u_o+u_F)/2$ in the sense of Pai's small perturbation concept.

Since we are dealing with the region close to the injector exit, we may assume that the expression

$$\varepsilon (x) = \varepsilon_{\infty} x$$

is to hold, so that equation (14) becomes:

$$\frac{\partial^2 Y_i}{\partial \eta^2} + 2\eta \frac{\partial Y_i}{\partial \eta} = -2x \left[\frac{w_i}{U\rho} - \frac{\partial Y_i}{\partial x} \right] \quad . \qquad (15)$$

The temperature may be determined in terms of the total enthalpy using the Crocco integral.

2C. The Distribution of Hydrogen Atoms in the Ignition Delay Zone.

We shall now study the influence of a given amount of radicals, produced upstream of the injector exit, on the ignition delay zone length.

In calculating the distribution of hydrogen atoms throughout this zone, we will make use of the simplifications mentioned in the two foregoing paragraphs.

If we insert (11) into (15) we are led to the following differential equation:

$$\frac{\partial^2 Y_5}{\partial \eta^2} + 2\eta \frac{\partial Y_5}{\partial \eta} - 2\xi \frac{\partial Y_5}{\partial \xi} + 2\xi f_1(\eta)\, Y_5 = -2\xi f_2(\eta) \qquad (16)$$

where

$$f_1(\eta) = \frac{K_3 \rho \frac{Y_3}{m_3}}{\left(K_3 \rho \frac{Y_3}{m_3}\right)_o}$$

and

$$f_2(\eta) = \frac{K_o \rho \frac{Y_2}{m_2} \frac{Y_3}{m_3}}{\left(K_3 \rho \frac{Y_3}{m_3}\right)_o}$$

are known functions of η , since ρ , T , Y_2 and Y_3 are calculated by solving the "frozen mixing" problem. The subscript o indicates the value corresponding to $\eta \to \infty$ (oxidizer side).

The chosen independent variables are defined as:

$$\xi = 2 \left(K_3 \rho \frac{Y_3}{m_3}\right)_o \frac{1}{U} x$$

$$\eta = \sqrt{U/2\epsilon_\infty}\, y/x \quad .$$

Equation(16)is linear in Y_5 , so that the influence of non-homogeneous boundary conditions, and the influence of the right hand side term with homogeneous boundary conditions may be considered successively.

Let us start with the effect of the introduction, in the mixing region, of oxygen atoms coming from the injector outer boundary layer. Due to reactions 1 and 4, each mole of atomic oxygen entering in the mixing zone must cause immediately the appearence of two moles of atomic hydrogen. This requirement gives the following integral continuity condition near the injector exit

$$I = \int_o^\infty \rho u \frac{Y_6}{m_6}\, dy = 2 \int_{-\infty}^\infty \rho u \frac{Y_5}{m_5}\, dy \quad . \qquad (17)$$

If we assume that the boundary layer thickness is small compared to the ignition delay length,we may write the initial distribution of Y_5 for the mixing region as a Dirac δ function of y , so that, close to $\xi = 0$, where the reaction term is negligible, Y_5 would be given by

$$Y_5 = N \frac{e^{-\eta^2}}{\xi} \quad ,$$

where, according to (17), N may be written as:

$$N = I \frac{\left(K_3 \rho \frac{Y_3}{m_3}\right)_o}{\beta (\rho u)_o \sqrt{2\pi \epsilon_\infty U}} \quad , \qquad (18)$$

β being a "non-uniformity factor" which takes into account the fact that ρu is not constant across the initial region of the mixing zone.

The effect of the non-homogeneous boundary conditions in the solution of the homogeneous differential equation obtained equating to zero the left hand side of (16) may be studied by solving the following equation:

$$\frac{\partial^2 X}{\partial \eta^2} - 2\eta \frac{\partial X}{\partial \eta} - 2\xi \frac{\partial X}{\partial \xi} + 2\xi f_1(\eta) X = 0 \qquad (19)$$

with the boundary condition

$$\xi = 0 \qquad X(0, \eta) = 1 \quad . \qquad (20)$$

The new function X is connected to Y_5 by the relation

$$X = \xi e^{\eta^2} \frac{Y_5}{N} \quad . \qquad (21)$$

The solution of (19) with the boundary condition (20), may be written as follows:

$$X(\xi,\eta) = 1 + \sum_{n=1}^{\infty} \xi^n X_n(\eta) \quad .$$

$X_n(\eta)$ being the finite solution of the Hermite equation

$$\frac{d^2 X_n}{d\eta^2} - 2\frac{dX_n}{d\eta} - 2n X_n = -2 f_1 X_{n-1} \quad . \qquad (22)$$

The equation corresponding to $n = 1$

$$\frac{d^2 X_1}{d\eta^2} - 2\eta \frac{dX_1}{d\eta} - 2X_1 = -2f_1 \quad . \qquad (23)$$

may be reduced to quadratures leading to:

$$X_1(\eta) = \sqrt{\pi}\, e^{\eta^2} \left[\operatorname{erfc}\eta \int_{-\infty}^{\eta} f_1 d\eta + \frac{1 + \operatorname{erf}\eta}{2} \int_{\infty}^{\infty} f_1 \operatorname{erfc}\eta \, d\eta - \right.$$

$$\left. - \int_{-\infty}^{\eta} f_1 \operatorname{erfc}\eta \, d\eta \right] \quad , \qquad (24)$$

where

$$\operatorname{erf}\eta = \frac{2}{\sqrt{\pi}} \int_0^{\eta} e^{-\beta^2} d\beta$$

$$\operatorname{erfc}\eta = 1 - \operatorname{erf}\eta \ .$$

It may be easily shown that:

$$\lim_{\eta \to +\infty} X_1(\eta) = \lim_{\eta \to +\infty} f_1(\eta) = 1 \ .$$

The remaining coefficients of the power series expansion are not so easily calculated, since the general solutions of the corresponding homogeneous differential equations are Hermite series. However they may be numerically calculated by using an iterative procedure consisting in writing (22) in the form:

$$\frac{d^2X_n}{d\eta^2} - 2\frac{dX_n}{d\eta} - 2X_n = -2\left[f_1 X_{n-1} - (n-1)X_n\right] \ . \quad (25)$$

To start with the iteration, a certain function is introduced instead of the X_n appearing in the right hand side of (25).

To find the behavior of X_n when $\eta \to +\infty$, we write:

$$\lim_{\eta \to +\infty} X_n(\eta) = \lim_{\eta \to +\infty} \left[f_1(\eta) X_{n-1}(\eta) - (n-1) X_n(\eta)\right] ,$$

so that

$$\lim_{\eta \to +\infty} X_n(\eta) = \frac{1}{n!}$$

Chosing as the starting function for the iterative process

$$X_n(\eta) = \frac{1}{n} X_{n-1}(\eta) \ ,$$

we obtain $X_n(\eta)$ with sufficient accuracy after four iterations

The main drawback of the power series expansion solution is its poor convergence; it is possible, however, to improve the convergence by means of the two successive steps:

a) We rewrite $X(\xi,\eta)$ as an exponential function

$$X(\xi,\eta) = \exp\left[\sum_{n=1}^{\infty} \xi X_n'(\eta)\right] ,$$

where

$$X_1'(\eta) = X_1(\eta)$$

$$X_2'(\eta) = X_2(\eta) - X_1^2(\eta)/2$$

$$X_3'(\eta) = X_3(\eta) - X_1(\eta)\, X_2(\eta) + X_1^3(\eta)/3$$

- - - - - - - - -

This development has the advantage that the first term gives the exact behavior of $X(\xi,\eta)$ when $|\eta|$ is large, what suggests that, for finite values of η, this expression would be more accurate that the power series expansion in terms of $X_i(\eta)$.

b) A further modification which may be useful, consists in recasting the power series into rational fractions. In our case, where only three terms have been computed, we may write $X(\xi,\eta)$ as:

$$\bar{X}(\xi,\eta) = \exp\left[\xi \frac{X_1 + \left(X_2' - \frac{X_1 X_3'}{X_2'}\right)}{1 - \frac{X_3'}{X_2'}\,\xi}\right] \qquad (26)$$

Figure 6 gives $X(\xi,\eta)/\xi e^{\eta^2}$ in the following particular case

u_o = 2000 m/sec $\quad T_o$ = 1300°K $\quad Y_{2o}$ = 0 $\quad Y_{3o}$ = 0.232

u_F = 1000 m/sec $\quad T_F$ = 900°K $\quad Y_{2F}$ = 1 $\quad Y_{3F}$ = 0

$$c_{po} = 1173 \text{ m}^2/\text{sec}^2\,°\text{K}$$

$$c_{pF} = 14937 \text{ m}^2/\text{sec}^2\,°\text{K}$$

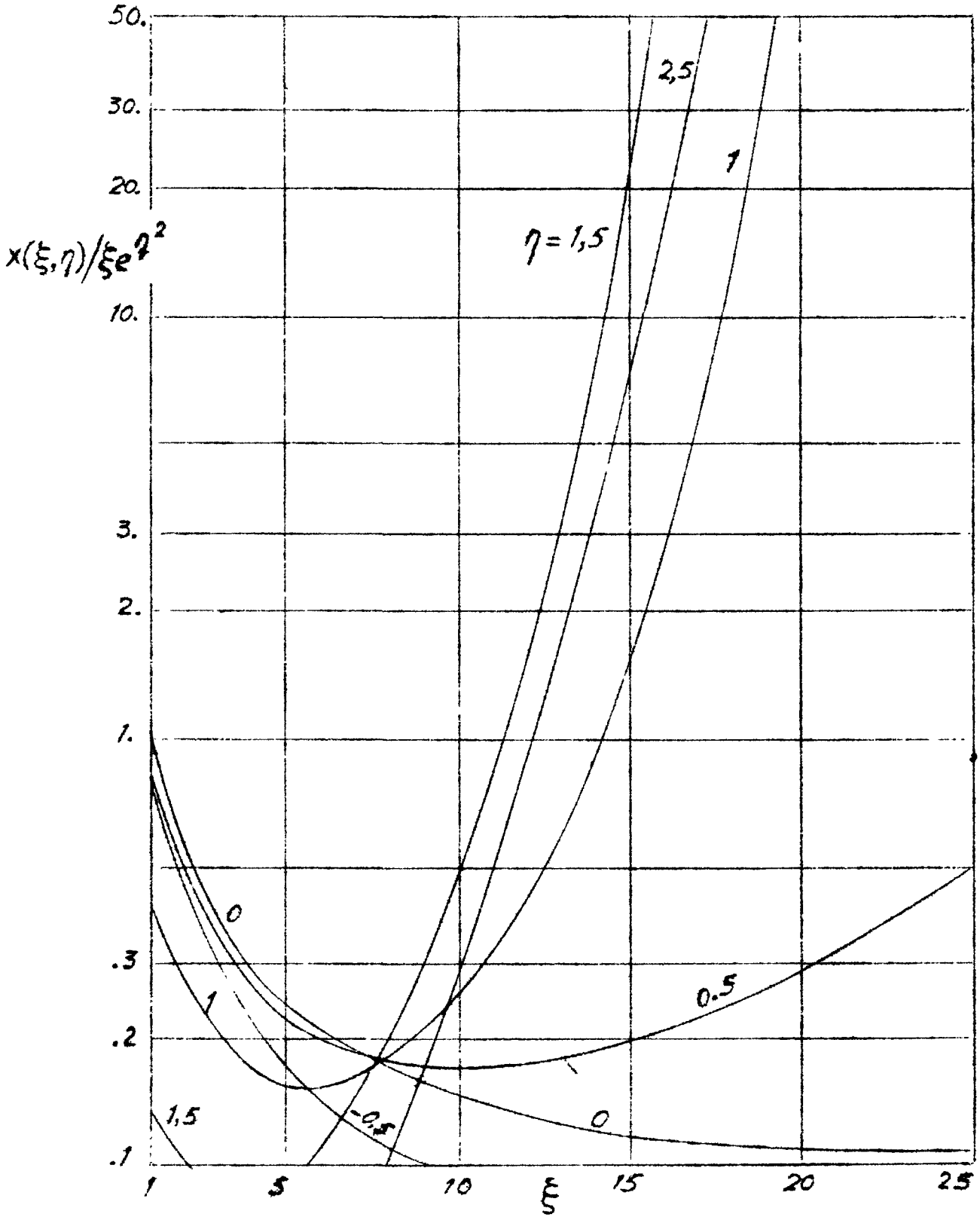

Fig 6. $X(\xi,\eta)$ versus ξ for different values of η

Concerning the solution of the non-homogeneous equation with homogeneous boundary conditions ($Y_5 = 0$ when $\xi = 0$ and when $\eta \to \pm \infty$), we tentatively assume a perturbation expansion in powers of ξ

$$Z(\xi,\eta) = \sum_{n=2}^{\infty} \xi^n \, Z_n(\eta) \quad ,$$

where $Z(\xi,\eta)$ is given by

$$Z(\xi,\eta) = \xi e^{\eta^2} Y_5 \quad , \tag{27}$$

and, as it can be verified by substituting in the complete differential equation and equating terms of like powers of ξ, the Z_n are defined by the following ordinary differential equations:

$$\frac{d^2Z_2}{d\eta^2} - 2\eta \frac{dZ_2}{d\eta} - 4Z_2 = 2f_2 e^{\eta^2} \quad , \tag{28}$$

and

$$\frac{d^2Z_n}{d\eta^2} - 2\eta \frac{dZ_n}{d\eta} - 2nZ_n = -2f_1 Z_{n-1} \quad ; \quad n > 2 \tag{29}$$

The function $Z(\xi,\eta)/\xi e^{\eta^2}$, is plotted in figure 7. This function has been calculated under the same particular conditions assumed to calculate $X(\xi,\eta)/\xi e^{\eta^2}$.

The solution of the complete non-homogeneous equation with non-homogeneous boundary conditions is given by

$$Y_5(\xi,\eta) = \frac{e^{-\eta^2}}{\xi} \left[N \, X(\xi,\eta) + Z(\xi,\eta) \right] \tag{30}$$

2D. <u>The Length of the Ignition Delay Zone</u>

We shall now study the influence of the dissociation in the injector outer boundary layer on the reduction of the ignition delay zone.

Let us begin estimating the amount of atomic oxygen

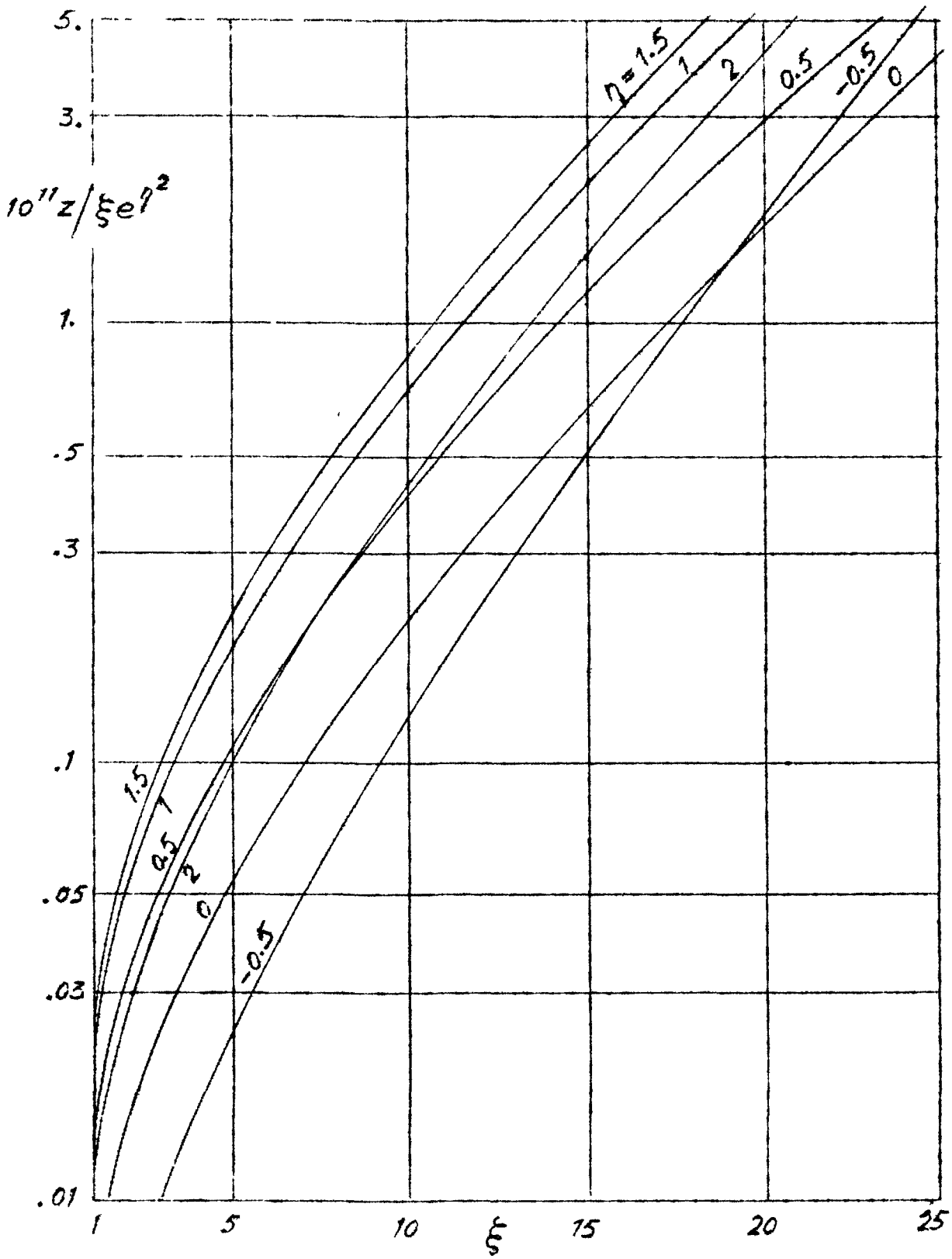

Fig 7. Z(ξ,η) versus ξ for different values of η

introduced in the mixing layer from the air stream. It must be pointed out that, althought the deceleration of the incoming air is limited as much as possible in order to avoid the air dissociation; some degree of dissociation in the injector boundary layer is in most cases unavoidable due to the high local temperature existing in that zone.

Figure 8, taken from [8], plots the maximum atomic oxygen concentration as well as the values of I versus the maximum temperature in the injector boundary layer. These curves have been calculated by following the method presented in [9].

In order to substantiate our approach, let us select the following values of the involved variables:

$$u_o = 2000 \text{ m/sec} \quad (*)$$

$$p = 10^4 \text{ Kg/m}^2$$

$$l = 0.25 \text{ m}$$

$$T_{max} = 2500^\circ K \quad .$$

From figure 8 we deduce

$$I = 0.175 \times 10^{-4} \text{ mole/sec. cm} \quad ,$$

while according to (18), with $\beta = 1$ and $\varepsilon_\infty = u/2\sigma^2$, $\sigma = 12$, we get

$$N = 0.980 \times 10^{-5} \text{ mole/gr} \quad .$$

Upon substituting this particular value in (30) and considering figures 6 and 7, it may be inferred that, in most cases of

---

(*) It should be noted that this value ought to be smaller than that corresponding to the outer boundary of the mixing layer due to the expansion taking place near the injector exit (See § 3 below); however since the aim of this computation is to gain some knowledge on the order of magnitude of the ignition delay length, the involved approximation is sufficient. Similar comment should be made concerning the pressure.

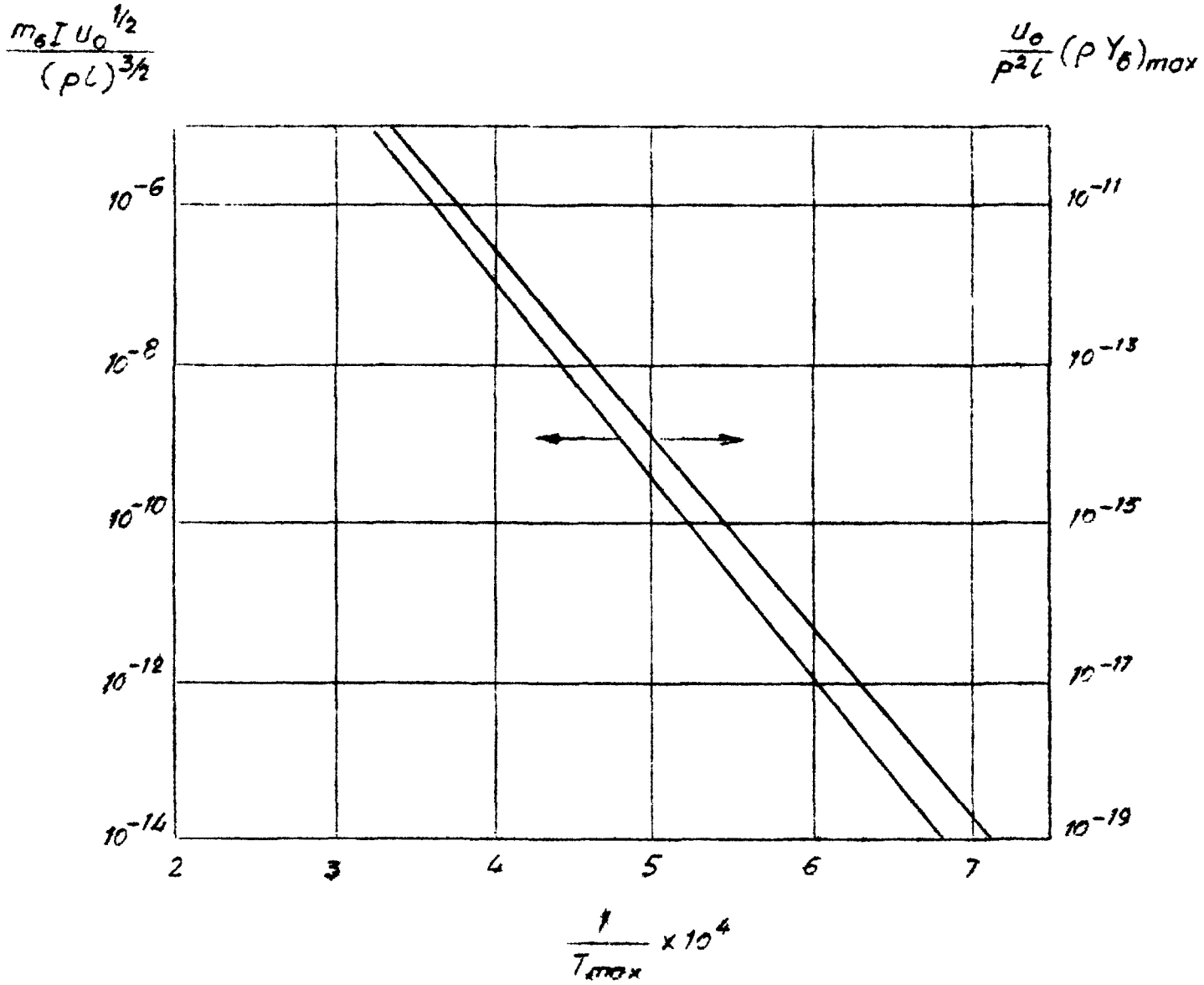

I in mole/sec.cm

ρ in Kg/m^2

l injector length in m

u_0 in m/sec

ρ in gr/cm^3

T_{max} in ^oK

Fig.8. Maximum atomic oxygen concentration in the boundary layer and amount of O introduced in the mixing layer, as a function of the maximum temperature in the boundary layer (from [8])

practical interest, dissociation in the injector outer boundary layer greatly accelerates the ignition process. As a matter of fact, for the above assumed values of u_o , p , and l , unless T_{max} becomes as small as $T_{max} = 1600°K$, reaction 0 is neglectable throughout.

Now, according to § 2A , we agree to define the end of the ignition delay zone as the value of ξ for which the reverse reaction 1 is of the same order as the forward reaction 3 at a local point η . Since the reverse reaction 1 has been neglected in this study, we will consider, consistently with this approximation that the ignition zone ends when

$$0.1\ K_3 \frac{Y_5}{m_5} \frac{Y_3}{m_3} = K_{-1} \frac{Y_1}{m_1} \frac{Y_5}{m_5} \quad , \qquad (31)$$

where the arbitrary factor 0.1, in the left hand side, is immaterial provided the slope of Y_5 versus ξ is large enough.

Since under the validity of our approximations we have

$$\frac{Y_5}{m_5} = \frac{Y_1}{m_1}$$

throughout the ignition zone, we get the maximum value:

$$\left(\frac{Y_5}{m_5}\right)_{max} = 0.1 \frac{K_3}{K_{-1}} \frac{Y_3}{m_3} \quad ,$$

where K_3/K_{-1} and Y_3/m_3 are known functions of η .

For a given value of ξ , the maximum Y_5 corresponds roughly to $\eta = 1$; then we deduce

$$\left(\frac{Y_5}{m_5}\right)_{max} \simeq 10^{-3} \quad .$$

Figure 6 indicates that this value is attained for values of ξ close to 20 , so that the expression

$$x_{max} = \frac{U}{\left(2K_3 \rho \frac{Y_3}{m_3}\right)_o} \xi_{max} \quad ,$$

together with the above assumed representative values, gives:

$$x_{max} = 2.3 \text{ cm.}$$

Notice that ξ_{max} is almost independent of p, hence x varies roughly as p^{-1}; the study of the influence of temperature on x_{max} is more complicated and deserves more extensive computations.

3. AERODYNAMIC FIELD NEAR THE INJECTOR EXIT

It is very interesting to study the feasibility of improving aerodynamically the mixing process and to diminish the ignition delay without appreciably disturbing the outer flow. When hydrogen is used as fuel, advantage may be taken of its low density.

Figure 9a, taken from[10], shows static pressure measurements along the jet axis when there is no injection and when the momentum of the fuel injected $\rho_F u_F$ is small compared with the outer flow momentum $\rho_o u_o$.

When there is no injection, the pressure distribution is that corresponding to a near wake behind an obstacle at supersonic speeds. Close to the base the pressure decreases due to the expansion fan formed when the streamlines are bent inwards, and it again increases, due to the formation of shock waves, when the streamlines approach the jet axis (Figure 9b). The adverse pressure gradients produce recirculation in the wake due to the fact that the fluid particles inside the mixing zone do not have enough total pressure and are obliged to bend backwards. Later on, these particles are entrained to the mixing zone and are replaced by new ones.

Figure 9a shows that when λ is small (which seems to be the case when hydrogen is used as fuel) the pressure distribution and the flow configuration outside the wake remain practically unchanged. Some experimental evidence seems to indicate that the near wake configuration is similar to what is shown in Figure 9c.

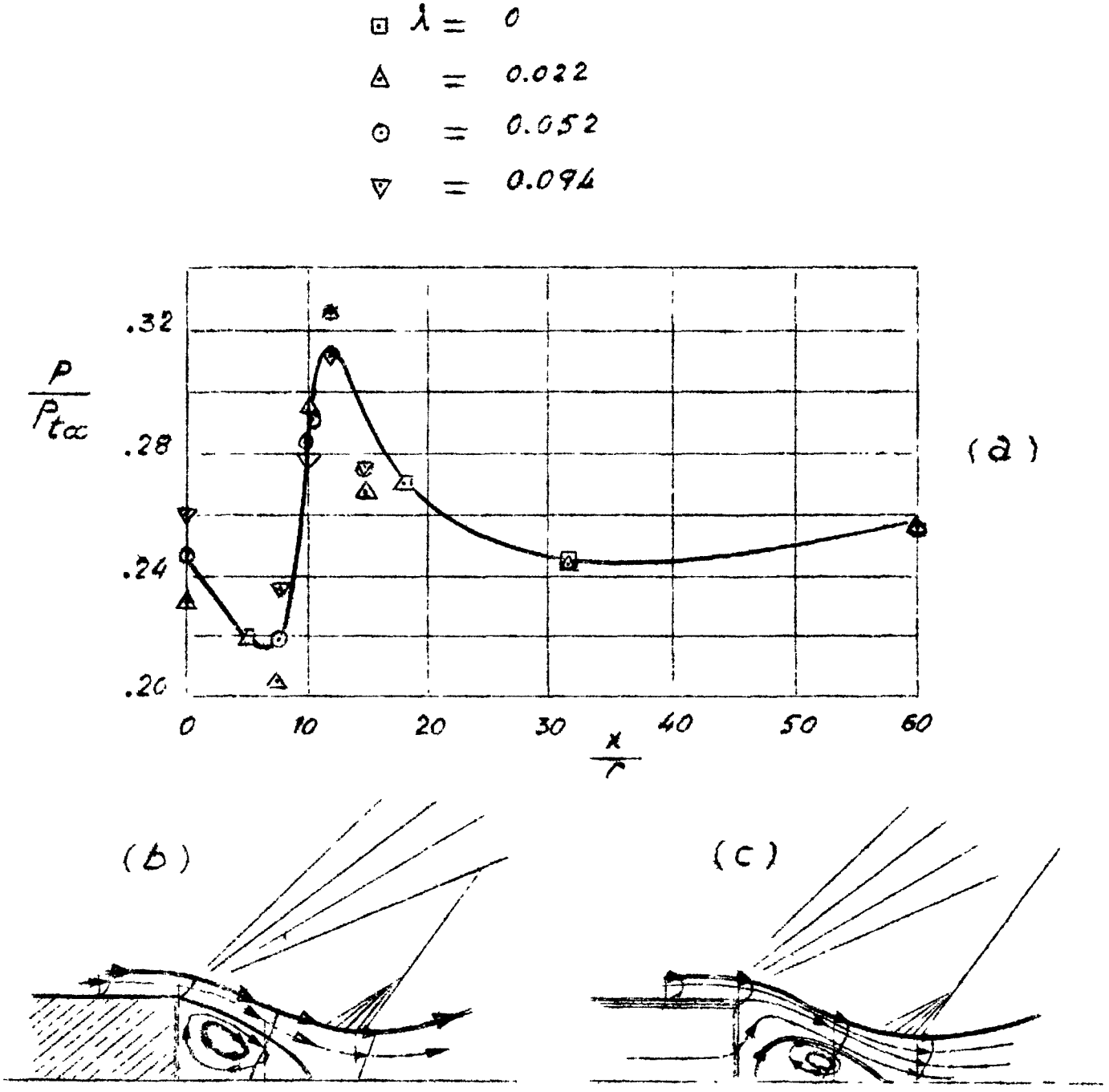

Fig 9. Wakelike configuration near the injector exit at low injection rates. $\lambda = \rho_F u_F / \rho_\infty u_\infty$.

(Fig 9a from[10])

When the total pressure of the fluid injected is small, the fuel cannot overcome the adverse pressure gradient along the axis, so that it bends outwards undergoing a process of mixing and recirculation. If the total pressure of the injected fuel goes up, the size of the recirculation bubble decreases very rapidly while the flow field outside the wake is not so greatly affected.

In those cases, in which the distance between separation and reattachment is comparable to the ignition delay length, recirculation sends radicals backwards, and these radicals, coming in contact with the hydrogen jet, trigger the fast reactions.

In order to gain an idea on the recirculation zone size, figure 10 shows some experimental measurements of the distance

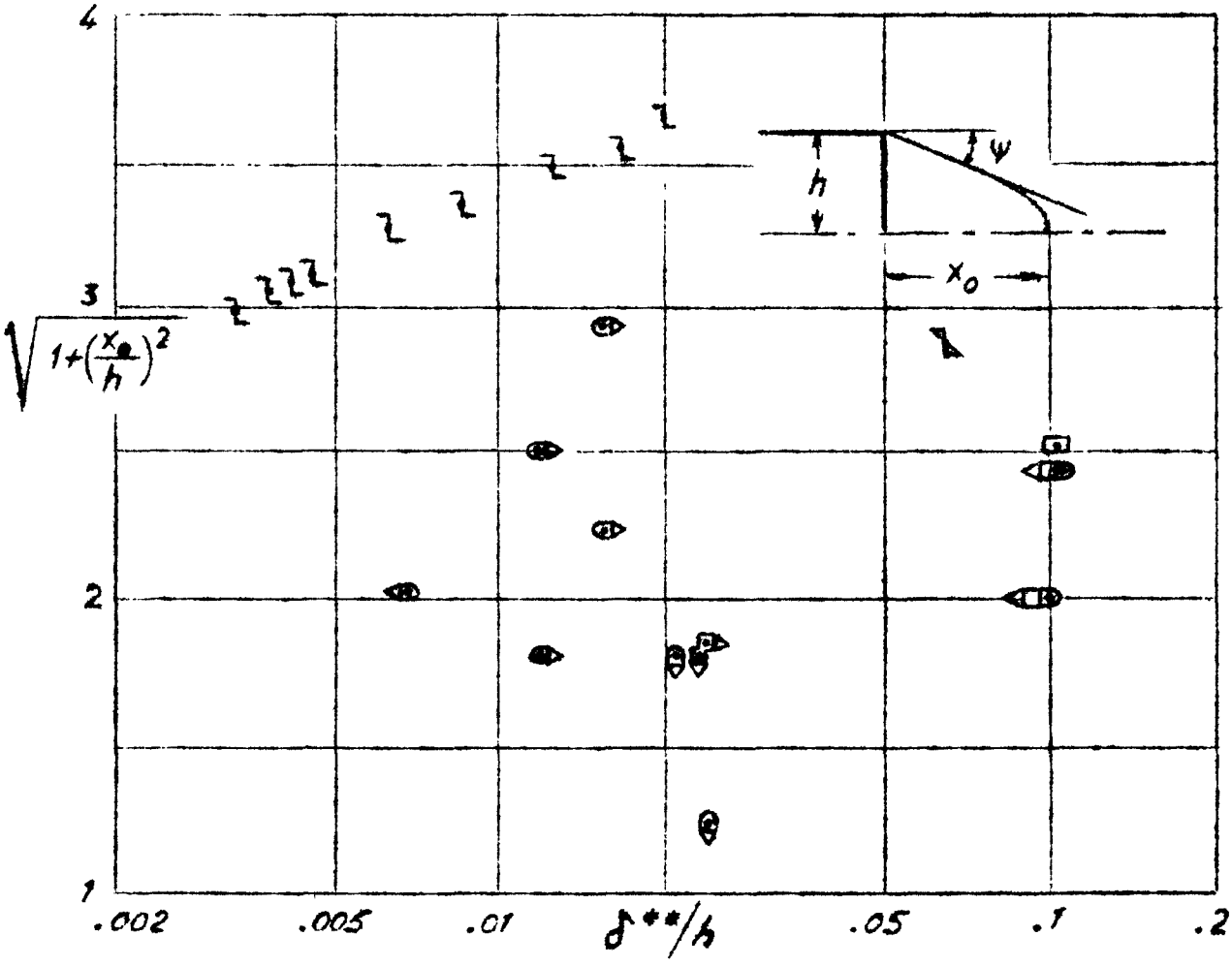

Fig 10. Recirculation zone length as a function of the boundary layer momentum thickness δ^{**} at the body shoulder.

between the separation point, placed in the body shoulder, and the downstream stagnation point, as a function of the boundary layer momentum thickness at the body shoulder. These experimental data correspond to two dimensional bodies, such as wedges and rearward facing steps; cilindrical bodies with the flow parallel to the cylinder axis, and slender axisymmetric bodies. The boundary layer is turbulent at separation. Data corresponding to laminar or near transitional separation have been sistematically excluded. One will note that the near wake length is always of the order of the injector diameter and no appreciable Mach or Reynolds numbers effects may be found. The data scattering is mainly due to the particular characteristic used to compute the position of the rear stagnation point when not measured directly. These characteristics are listed in the following table.

Symbol	Body	Reference	Method used to calculate x_o
	Rearward-facing step	11	Inflection point in the centerline static pressure distribution.
	Cone-cylinder	12	Direct measurement
	Prism	12	Direct measurement
	Rearward-facing step	13	$x_o = h \tan \psi$
	Cone	14	End of plateau in the centerline total temperature distribution
	Wedge	14	End of plateau in the centerline total temperature distribution
	Cone	15	Direct measurement
	Blunt cone	16	Wake shock origin

Similar data in the case of injection into the base region

are rather scanty and limited in scope, so that we shall make use of some theoretical results wich are valid for the two dimensional base zone under low injection rate conditions.

3A. Influence of the Injection on the Recirculation Zone Length

The configuration of this zone is studied using essentially the theory by Korst et al[17], who consider the following phenomena:expansion around the body shoulder or injector exit, turbulent mixing at constant pressure along the wake boundaries, pressure rise at the wake neck, and mass conservation inside the wake. In order to study the mixing process, Korst uses the somewhere else mentioned small perturbation scheme to reduce the momentum equation, along the dividing streamline, to the heat conduction equation. No consideration has been given up to now to the mixing of widely different gases.

To solve the problem,we tentatively assume a turning angle ψ and calculate from the outer inviscid flow the Mach number M_o at the outer boundary of the mixing layer and the reattachment pressure p'. For a particle along a streamline within the mixing layer to be able to overcome the pressure rise through the reattachment zone and to pass downstream, its total pressure must be greater than the terminal static pressure p'. The dividing streamline separates these particles from those unable to leave the recirculation zone. The static pressure in this zone is determined by requiring that the total pressure along the dividing streamline, as it approaches the reattachment zone under almost isentropic recompression conditions, be equal to the terminal static pressure. For the steady case, without injection or suction, the dividing streamline at separation as calculated from the mixing layer theory must also be a dividing streamline at reattachment, otherwise fluid would be either continually removed or injected from the inner wake.

In the case of small injection rates, Carrière[13] relates the turning angle ψ with the outer Mach number M_o and a

generalized mass injection coefficient c_q by means of the following linearized expression

$$\psi (M_o , c_q) = \psi (M_o, 0) + c_q \left(\frac{\partial \psi (M_o, c_q)}{\partial c_q}\right)_{c_q=0} \qquad (32)$$

where c_q is defined in the following way:

$$c_q = \frac{q}{\rho_o u_o L} \left(1 - \frac{u_j}{u_o}\right) + \frac{\delta^{**}}{L} \qquad (33)$$

and

q = Mass rate injected in the inner wake per unit span

$L = \sqrt{h^2 + x_o^2}$ = Distance between separation and reattachment

δ^{**} = Momentum thickness of the injector outer boundary layer at the injector exit

u_o = Air velocity at the outer boundary of the mixing layer

u_j = Axial component of the injection velocity

Figure 11 gives $\psi (M_o, 0)$ and $\partial\psi/\partial c_q$ as calculated by Carrière.

It is interesting to discuss whether a linear treatment would be appropriate to study the aerodynamic field near the injector exit in the cases of practical interest. A simple numerical analysis indicates that, provided hydrogen is used as fuel, the values of c_q involved are small enough to justify such a simplification.

Let us assume for instance a value of $L/h = 2.5$. The first term of the right hand side of (33) takes the following value:

$$\frac{\rho_F u_F 2h}{\rho_o u_o L} \left(1 - \frac{u_F}{u_o}\right) = 0.0181,$$

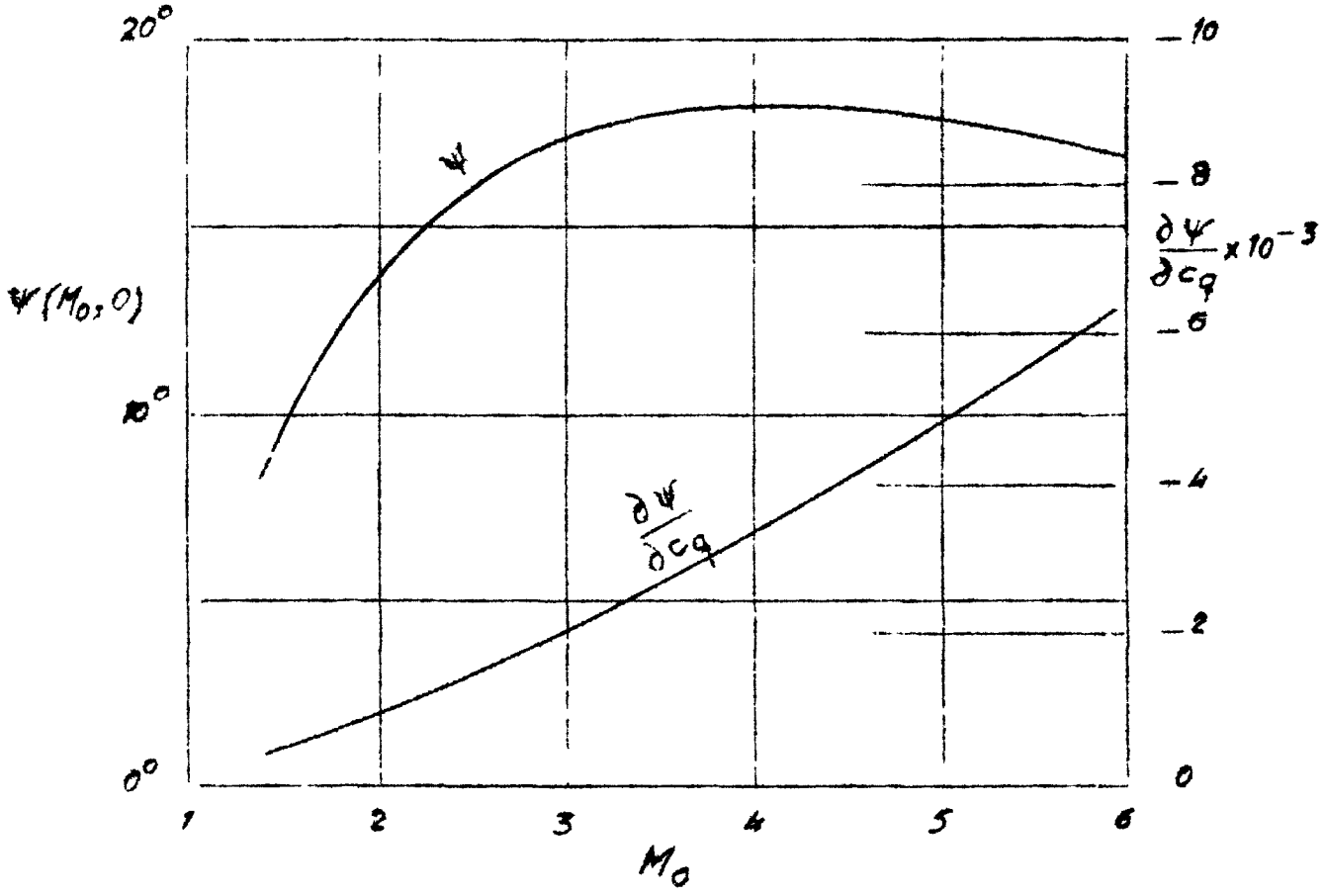

Fig 11. Ψ and $\frac{\partial \Psi}{\partial c_q}$ as a function of the outer Mach number M_o (from [13])

while the second term δ^{**}/L is normally smaller.

Since in our case is $M_o = 2.75$, we get from figure 11 $\partial\psi/\partial c_q = -1.8$, hence the hydrogen injection deflects the dividing streamline by an amount of only 0.03°.

In conclusion, the simple calculations presented strongly support the evidence that recirculation controls the flow pattern near the injector exit, and in many cases the ignition delay length. However much more theoretical and experimental work must be done.

R E F E R E N C E S

1. Burke, S.P. and Schumann, T.E.W. : "Diffusion Flames". Ind. Eng. Chem. 20 pp 998-1004 (1928).

2. Da-Riva, I. : "The Internal Structure of Hydrogen-Air Diffusion Flames" Will appear in Astronautica Acta. July-August 1966.

3. Wooldridge, C.E. and Muzzy, R.J. : "Measurements in a Turbulent Boundary Layer with Porous Wall Injection and Combustion". Tenth Symposium (International) on Combustion (The Combustion Institute, Pittsburgh 1965) pp 1351-1362.

4. Van Dyke, M. : "Perturbation Methods in Fluid Mechanics" (Academic Press New York and London 1964) Chap V pp 77-97.

5. Stull, F.D. : "Scramjet Combustion Prospects" Astronautics & Aeronautics 3 12 pp 48-52 (1965)

6. Korst, H.H., Page, R.H. and Childs, M.E. : "Compressible Two-Dimensional Jet Mixing at Constant Pressure" University of Illinois ME Technical Note 392-1 (1954)

7. Korst, H.H. and Chow, W.L. : "Non-Isoenergetic Turbulent ($Pr_t = 1$) Jet Mixing between Two Compressible Stream at Constant Pressure" NASA CR-419 (1966)

8. Liñán, A., Urrutia, J.L. and Fraga, E. : "On Diffusive Supersonic Combustion" Fifth ICAS Congress London (England) (1966).

9. Rae, W.J. : "A Solution for the Non-equilibrium Flat Plate Boundary Layer" AIAA J. 1 10 pp 2279-2288 (1963).

10. Zakkay, V. and Krause, E. : "Mixing Problems with Chemical Reactions". In "Supersonic Flow, Chemical Process and Radiative Transfer". Ed. by D.B.Olfe and V. Zakkay (The Mac Millan Co. New York 1964) pp 3-29.

11. Thomann, H. : "Measurements of Heat Transfer and Recovery Temperature in Regions of Separated Flow at a Mach Number of 1.8".
F.F.A Report 82 Stockolm (1959).

12. Badrinarayanan, M.A. : "An Experimental Investigation of Base Flows at Supersonic Speeds"
J.Roy.Aer.Soc. 65 607 pp 475-482 (1961)

13. Carrière, P. : "Recherches Récentes Effectuées a L'O.N.E.R.A. sur les Problèmes de Recollement"
7eme Symposium de Mécanique des Fluides Jurata (Pologne)(1965)

14. Todisco, A. and Pallone, A. J. : "Near Wake Flow Field Measurements"
AIAA J. 3 11 pp 2075-2080 (1965)

15. Martelluci, A., Trucco, H. and Agnone, A. : "Measurements of the Turbulent Near Wakes of a Cone at Mach 6"
AIAA J. 4 3 pp 385-391 (1966).

16. Waldbusser, E. : "Geometry of the Near Wake of Pointed and Blunt Hypersonic Bodies"
AIAA J 4 10 pp 1874-1876 (1966).

17. Korst, H.H., Page, R.W. and Childs, M.E. : "A Theory for Base Pressure in Transonic and Supersonic Flow". Univ. of Ill. Eng. Exp. Sta. ME-TN-392-2; also OSR-TN-55-89, Contract No AF 18 (600)-392, March 1955.

- - - - - - -